

Exploring archaeological landscapes using drone-acquired lidar: Case studies from Hawai'i, Colorado, and New Hampshire, USA

Jesse Casana ^{a,*}, Elise J. Laugier ^a, Austin Chad Hill ^e, Kelsey M. Reese ^b, Carolin Ferwerda ^a, Mark D. McCoy ^c, Thegn Ladefoged ^d

^a Department of Anthropology, Dartmouth College, USA

^b Department of Anthropology, University of Notre Dame, USA

^c Department of Anthropology, Southern Methodist University, USA

^d Department of Anthropology, University of Auckland, New Zealand

^e Department of Anthropology, University of Pennsylvania, USA



ABSTRACT

Although aerial lidar has proven to be a powerful tool for mapping archaeological landscapes, particularly in forested regions of the world, the high costs of conventional lidar acquisition from aircraft or professional-grade drones remains a hurdle to many researchers. The recent development of ultra-compact, relatively low-cost lidar mapping systems that can be deployed on consumer-grade drones now make it feasible for archaeologists to collect their own high-resolution aerial lidar of sites and landscapes, but the efficacy of these systems remains largely untested. This paper presents results of surveys undertaken using a ultra-compact, drone-deployed lidar at archaeological sites located in three different environments: 1) tropical forests at Kealakekua Bay State Historic Park, Hawai'i, 2) piñon-juniper forest on Mesa Verde's North Escarpment, Colorado, and 3) mixed deciduous-evergreen forest at Enfield Shaker Village, New Hampshire. Results reveal a wealth of archaeological features at the three study sites and demonstrate the potential of drone-based lidar as a tool in archaeological prospection, but also illustrate some of the significant technical and practical challenges involved in making use of this exciting emerging technology.

1. Introduction

The past decade has witnessed a revolution in archaeologists' ability to discover and interpret the remains of past human activities in forested and densely vegetated areas of the world, largely due to the increasing availability and steadily improving resolution of aerial lidar. Forests have confounded archaeological investigations for decades, as conventional pedestrian survey methods have difficulty accessing and recognizing archaeological remains, surveying tools like GPS and Total Stations are difficult to operate, terrestrial geophysics is nearly impossible, and traditional forms of aerial or satellite remote sensing rarely reveal features hidden below tree canopy. Because aerial lidar offers the ability to record the ground below trees and other vegetation, producing a "bare earth" digital terrain model (DTM), it can reveal any archaeological feature that has topographic expression, including building remains, earthworks, agricultural field systems, canals, and roadways (Opitz and Cowley, 2013). As such, aerial lidar has rapidly become a transformative tool, especially in areas that are densely forested or vegetated such as central America (e.g., Chase et al. 2011; 2012; 2014a; 2014b; Chase and Weishampel 2016; Fisher et al. 2016; Golden et al.

2016; Inomata et al. 2017; Loughlin et al. 2016; Macrae and Iannone 2016; Prufer et al. 2015; Rosenswig et al., 2013; Stenborg et al. 2018; Venter et al. 2018; Yaeger et al. 2016), Europe (e.g., Bewley et al., 2005; Cerrillo-Cuenca 2017; Challis et al. 2011; Due Trier et al. 2015; Masini et al. 2018), North America (e.g., Gallagher and Josephs 2008; Henry et al. 2019; Johnson and Quimet 2014; Randall 2014; Riley and Tiffany 2014; Krasinski et al. 2016), Southeast Asia (Evans et al. 2013; Evans and Fletcher 2015), and other parts of the world (e.g., McCoy et al. 2011; Opitz et al. 2015; Freeland et al. 2016; Cheng et al. 2016).

The main stumbling block faced by researchers interested in using aerial lidar for archaeological exploration is the high costs associated with data collection. Conventional airborne lidar sensors are bulky instruments that are very expensive and require specially outfitted planes to deploy, such that archaeologists must generally contract with a lidar firm to perform data collection, a cost-prohibitive option to most researchers. Alternatively, data is sometimes distributed by government agencies, but it is rarely available at better than 1 m resolution and is limited in coverage or unavailable in many areas. In recent years, more compact lidar sensors have made drone-acquired lidar possible for the first time and several recent studies have demonstrated the potential for

* Corresponding author at: Department of Anthropology, Dartmouth College, Hanover, NH 03755, USA.
E-mail address: jesse.j.casana@dartmouth.edu (J. Casana).

archaeological documentation using data these systems produce (e.g., Khan et al. 2017; Murtha et al. 2019; Risbøl and Gustavsen 2018). But deploying survey grade lidar has many of the same shortcomings as other airborne systems. The instruments remain too costly for all but the most well-funded researchers, while the size and weight of even the smallest survey-grade aerial lidar instruments are such that they require professional-grade drones (weighing > 25 kg/55lbs) to carry them.

A new generation of ultra-lightweight (<3.5 kg), relatively low-cost lidar sensors are now available, largely developed for use in “simultaneous localization and mapping” (SLAM) employed in autonomous vehicles. Recently, numerous firms have sought to integrate these sensors into drone-deployable mapping packages. For the first time, archaeologists are thus able to collect our own lidar data using a small sensor mounted on a standard, consumer-grade drone for a cost comparable to other field research instruments (e.g., VanValkenburgh et al. 2020). As with the revolution that drones have made possible in visible, near-infrared and thermal imaging (e.g., Casana et al., 2020; Hill et al. 2020; Casana et al., 2017; McLeester et al., 2018), these new systems offer a range of exciting opportunities for archaeological discovery and mapping because we can collect lidar data where and when it is needed, and at whatever resolution is appropriate to maximize feature recognition. Nevertheless, the relatively new set of instruments and technologies needed to undertake drone-based lidar surveys remain largely untested in archaeological contexts.

This paper presents a summary of our recent experiments with drone-based lidar, discussing results from surveys at archaeological sites possessing a variety of cultural features located across a range of different environmental zones. We have conducted surveys at: 1) a

traditional (pre-European contact) royal center located in tropical forests at Kealakekua Bay State Historic Park, Hawai'i, 2) an ancestral Pueblo community in piñon-juniper forest on Mesa Verde's North Escarpment, Colorado, and 3) a historical Shaker Village site located in a mixed deciduous-evergreen forest in Enfield, New Hampshire (Fig. 1). We have developed a set of field methods for data acquisition and experimented with a variety of post-processing approaches to achieve optimal results using relatively low-cost drone-based lidar systems. Results reveal an abundance of archaeological features at all the sites, including both known and previously unrecorded features, providing a strong basis for ongoing research in these areas. More broadly, our results offer a blueprint for archaeologists interested in deploying drone-based lidar in their own research projects, helping to outline the opportunities, limitations, and ongoing challenges with this exciting emerging technology.

2. Instrumentation and methods

Collection of drone lidar data requires a significant number of different instruments (Fig. 4A) and limitations in current commercial technologies mean that drone lidar surveys are far more complex than visible light-based imaging or photogrammetric mapping (Fig. 4B). Building and deploying a low-cost, drone-based lidar system for archaeological survey requires a number of decisions that fall into three categories: 1) hardware (lidar, drone), 2) data collection (flight plan, altitude), and 3) post-processing (data processing, visualization). Below we describe the system we created and some of the pros and cons that had to be weighed in terms of functionality and cost.

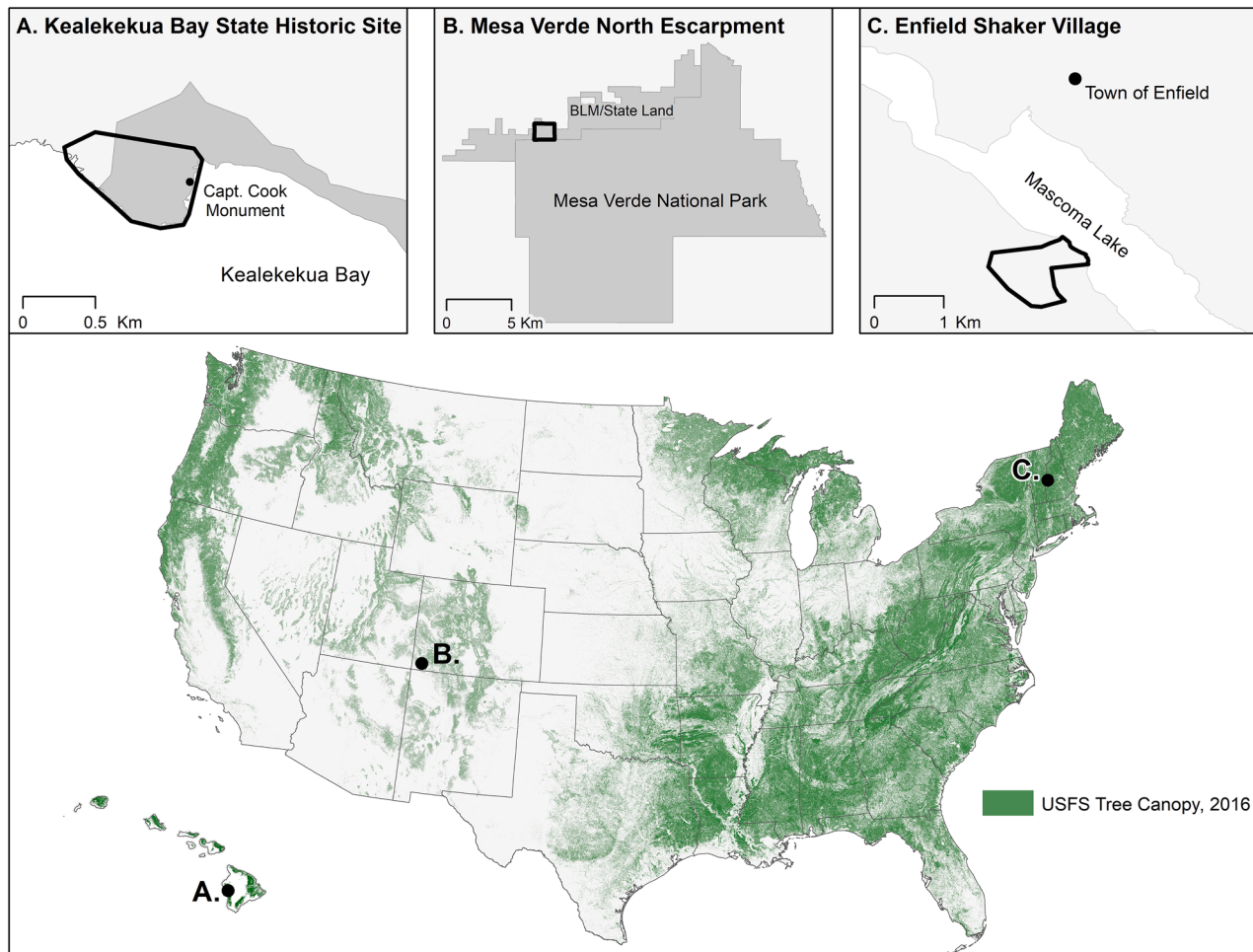


Fig. 1. Locator map, showing the three study sites in this paper and areas of the United States covered by tree canopy (courtesy United States Forest Service, 2016).

2.1. Hardware

2.1.1. Lidar

An aerial lidar survey system involves several key components including the lidar sensor that records angular and distance measurements, an inertial measurement unit (IMU) that records orientation information for each measured point, a precise GNSS (Global Navigation Satellite System) system to record location information for each point, and a drone or other vehicle on which the system can be deployed. Most commercially available drone-deployable lidar systems are sold by “integrators” who package third party lidar sensors and IMUs into a composite drone-deployable instrument, capable of producing a single fused data product. While many companies have begun to offer these integrated drone lidar packages, most use one of just a few commercially available lidar sensors that are sufficiently small and light to be carried on a consumer-grade drone.

We use a lidar package that is built around the Velodyne “Puck” VLP-16 lidar, one of the most popular sensors for its small size, light weight, and affordable price tag, integrated with a proprietary Geo-MSS Navigator IMU, designed and built by San Diego-based Geodetics Inc. (Fig. 2). The Velodyne lidar series is designed for SLAM sensing from vehicles, and thus has several shortcomings compared to more costly survey-grade lidar systems. While lidar systems designed for mapping typically have a rotating mirror or set of mirrors, the Velodyne VLP-16 has 16 hard-mounted lasers that rotate, collecting data in a 30°

vertical field of view. The VLP-16 has a relatively low power laser that limits its effective range to 70–80 m, restricting the height at which it can be flown. It collects around 300,000 points per second, which is much lower than more costly survey systems that can collect more than a million points per second. Moreover, while some systems offer the possibility of full wave-form lidar data, which enables a range of more sophisticated analyses (Mallet and Bretar 2009), or at least multiple returns per pulse, the VLP-16 is limited in its ability to penetrate dense tree canopy by offering only two returns per pulse. The VLP-16 records the strongest and the last return, which often corresponds to the tree canopy and the ground, but is nonetheless a serious limitation as compared to more costly sensors.

Velodyne offers several other lidar sensors that can be integrated in the same manner as the VLP-16 we use in this study, such as the HDL-32E which has twice as many lasers and thus doubles the speed of data collection for the same point density, as well as the HDL-32C, which additionally doubles the strength of the pulse to allow for measurements at greater distances, but these systems also cost more than double the price of the VLP-16. Systems such as the Reigl mini-VUX line of lidar sensors offer the additional advantage of either full waveform returns or up to five returns per pulse, and significantly greater range, improving canopy penetration and survey efficiency, but are prohibitively expensive for many researchers. Moreover, the larger size of Reigl lidar sensors are above the payload capacities of the largest consumer-grade drones currently available, and thus require larger custom enterprise drones or aerial vehicles such as Riegl's own RiCOPTER, which increase the logistical problems of transportation and field deployment.

2.1.2. Drone and GNSS

The Geodetics MMS lidar system is designed to be flown on the DJI Matrice 600 (M600) hexacopter (Fig. 2), the largest drone currently sold by industry leader DJI and the current industry standard for high payload operations, with payload capacity at 6 kg (13lbs). The M600 has not seen a redesign since it was originally released in 2016, when *Wired* magazine called it, a “six-rotor pro-level monster drone that looks like it spends nights and weekends hunting for Sarah Connor” (Barrett 2016), and it certainly lacks many of the upgrades that are common on newer DJI models, such as obstacle detection and extended flight times. The smallest third party commercial case available for the M600 is still more than a meter square, falling just below the maximum luggage weight and size many airlines will accept.

Flying drone lidar requires balancing the power and navigation needs of both the platform (i.e., drone) and the instrument (i.e., lidar). A single M600 flight requires six batteries, and given the weight of the lidar system, flight times are only 12–15 min depending on altitude and wind conditions. In order to mount the lidar system on the drone, it requires a customized frame. The instrument is not integrated into the drone software, power, or navigation systems, and thus it necessitates its own batteries and its own GPS/GNSS sensors.

In order to effectively post-process lidar data Geodetics MMS, it is necessary to simultaneously collect GNSS data using a ground-based instrument (Hill et al., forthcoming). During our surveys, we use an iGage 3 static GNSS receiver, which is set up and allowed to run continuously during surveys. Data collected by the instrument is then used as the basis for post-processing of lidar data (see below).

2.2. Data collection

To effectively collect drone-based lidar, careful consideration must be given to mission planning parameters in terms of altitude, speed, and other factors. Many archaeologists will be familiar with conventional drone-based aerial imaging in which a higher altitude produces a larger footprint on the ground at the cost of lower resolution. With a low-cost lidar system, attenuation of the pulse beam strength beyond 75 m means that the effective width of the data collected on the ground is reduced at higher altitudes (Fig. 3). For example, if a survey is flown at 40 m above

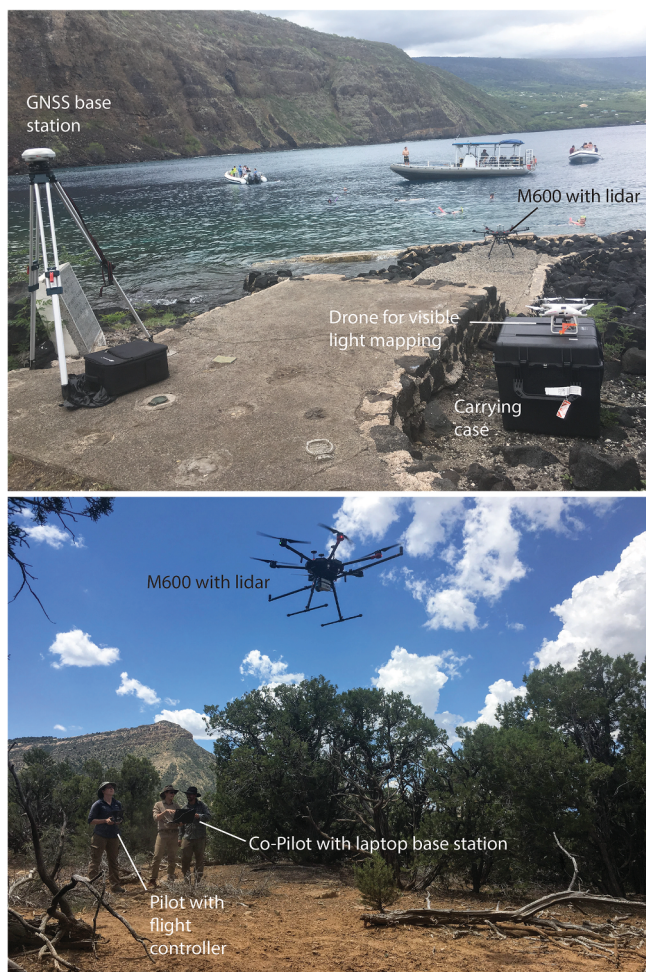


Fig. 2. DJI Matrice 600 drone with Geodetics Geo-MSS Navigator lidar system, incorporating a Velodyne VLP-16 lidar and 2-m boom for GNSS antennas. Surveys also require a static iG3 GNSS receiver and a laptop broadcasting mobile WiFi for flight mission planning and execution.

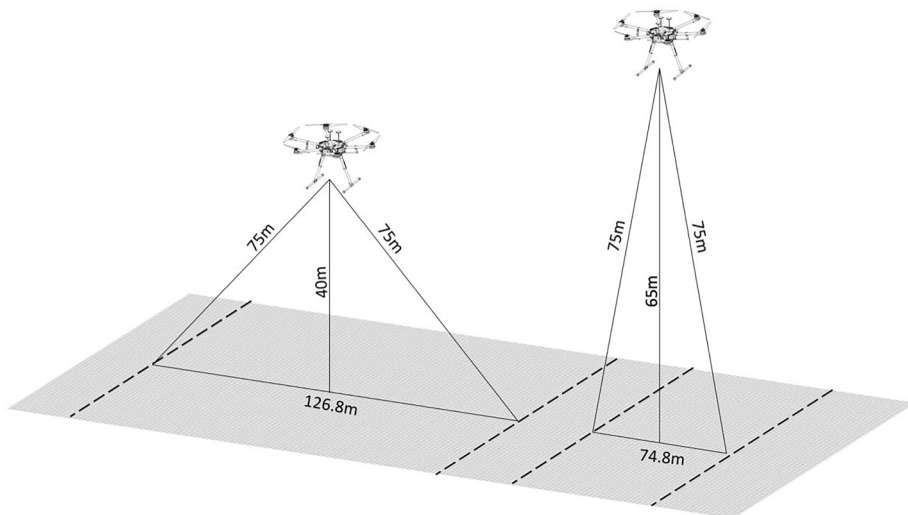


Fig. 3. Diagram illustrating trade-offs between lidar swath-width and the altitude of the sensor. Attenuation of the laser beam restricts the effective altitude at which surveys can be conducted.



Fig. 4. A) Aerial photo of Ka'awaloa, a forested peninsula in Kealakekua Bay, Hawai'i, that was home to a large royal center and settlement. B) Stone architectural remains on the Ka'awaloa Peninsula are covered by dense tropical forest (Photos by Jesse Casana; Mark McCoy for scale).

the ground, the maximum swath width would be 126.8 m with decreasing resolution and accuracy at the margins, while at 65 m altitude, swath width is only 74.8 m, but with reduced loss in accuracy and resolution. Thus, there is both a maximum altitude at which the sensor can be operated, but also a decreasing efficiency as that maximum is approached, due to the narrowing of the swath width. On the other hand, unlike aerial surveys designed to collect images for photogrammetric processing in which overlapping images of greater than 75% are

optimal, it is only necessary to have a relatively small (<10%) overlap between survey transects in a lidar mission plan in order to ensure complete coverage of the resulting point cloud. However, in our experience, overlapping transects by greater than 50%, such that all parts of the ground can potentially be imaged from at least two survey transects, will produce better results when attempting to penetrate tree canopy or other forms of vegetation. Most of our flights were conducted at 40 m altitude, providing a good compromise between coverage and point density while enabling us to remain above tree canopy in most instances.

We plan surveys using UgCS, a powerful but complicated mission planning software. While more cumbersome than the numerous app-based, third-party mission planners now available, UgCS offers several key advantages that are necessary for lidar flights, particularly with instruments like the Geodetics MMS that require calibration after takeoff. UgCS enables each individual waypoint in a survey to be independently positioned, it enables drone speed, orientation, and altitude to be changed for each flight segment, and critically, it enables the drone to follow changes in topography using either an SRTM or user-supplied basemap such that the lidar sensor remains within its effective range of the ground. On the downside, UgCS requires missions to be planned on a laptop, and then transferred to the drone, while flights themselves are monitored on a tablet, requiring a WiFi connection between the tablet and the laptop. The complexity of the operation means that it requires a ground crew of at least two people to execute flights safely and efficiently. A typical lidar drone survey generally begins with a calibration flight pattern in which the IMU configures itself, and for the Geo-MSS Navigator, calibration involves making at least four 90° turns with the drone while in flight or by performing a figure-eight maneuver prior to beginning data collection. Once calibration is complete, typically requiring 1–2 min of flight time, the drone can then proceed on a data collection mission.

Speed is a key limitation as the faster the drone is moving during survey, the lower the recorded point density on the ground. In cases where there is little vegetation obscuring the ground, it is possible to fly at 4–5 m/s and still achieve usable results, but when penetration through vegetation is the goal of a survey, flight speeds during data collection must be limited to 2 m/s or less. These very slow speeds, combined with relatively low working altitudes, greatly limit the overall area that can be effectively surveyed in a single flight. In order to improve survey efficiency, we plan missions such that the calibration phase of the flight, transit to and from a target area, and transit between end points of survey transects are all flown at higher speeds, enabling us to cover more area with a single flight.

Because each flight requires six large, TBS47 or TBS48 batteries, transporting and maintaining them can be challenging in remote field conditions. While the TBS48 batteries offer slightly more power, the TBS47 is designed to be just under the 100 W/hour limit for transporting in unlimited quantities in carry-on baggage on most airlines. In our experience the benefit in terms of additional flight time provided by the larger TBS48 batteries is negligible, so that the TBS47 are preferred. When conducting surveys, we maintain three sets of batteries such that one can begin charging as soon as a flight is completed, enabling us to fly throughout the course of a day with relatively little interruption. However, the batteries get very hot during flight and require time to cool before they can be recharged, and in very warm weather as we experienced in Mesa Verde, they will cool more slowly and require more time to begin recharging. Additionally, in cold and windy weather, as we experienced in New Hampshire, the batteries will not work at all unless kept warm, as they do not contain the built-in warming system of more advanced DJI batteries. When working in remote areas that do not have available power outlets for charging, we rent a portable generator, and we found that to charge twelve batteries simultaneously requires at least a 2200 W unit.

2.3. Post-processing

2.3.1. 3D point data processing

Raw data from the Geo-MMS sensor is downloaded after a mission and processed, along with GNSS base station data, in a proprietary software package from Geodetics Inc. to produce a standard georeferenced .las point cloud. Sets of point clouds from a complete survey are further processed in a combination of the widely used LAStools suite of powerful command line tools (Isenburg 2011, rapidlasso.com) along with the open source SAGA GIS (www.saga-gis.org/en/index.html) and CloudCompare (www.danielgm.net/cc/) packages (Hill et al., forthcoming). This further processing is done to combine multiple point clouds into a single composite, remove noise, check for errors, classify points into the standard classification system (including ground, vegetation, building, etc.), and convert the “ground” classified points to a “bare earth” DTM that represents the surface with all buildings and vegetation removed.

These final steps, classifying the point clouds and producing the DTM, are the most critical step for revealing anthropogenic features hidden below vegetation, and there are a variety of workflow options for classifying point clouds. One important limitation of sensors intended for SLAM, including the Puck series like the VLP-16, is a significant amount of “noise” relative to survey-grade sensors like those from Riegl. The sensor is claimed to have accuracy up to +/- 2 cm, but with the additional error of the IMU and the GNSS sensors combined with the movement of the drone platform, the errors in each point can be significant, making classification more challenging (Hill et al., forthcoming).

2.3.2. Visualization

After the creation of the final, composite, cleaned, and classified point clouds and the generation of bare earth DTM data, the resulting geo-tiffs can be visualized in a variety of ways. For inspecting and sharing the raw data, we use the free Potree package (Schuetz 2016) to visualize the classified point cloud data and share it with colleagues and stakeholders over the internet via a web browser. Although it can be cumbersome, it provides an easy way to show people the extent and density of the raw data. The DTM outputs are then brought into GIS software and visualized in a number of ways, with the specific approaches in each case study selected in order to highlight the subtle topographic anthropogenic features we are interested in identifying. Additional DEM processing can be done with SAGA GIS and the Relief Visualization Toolkit (Kokalj and Somrak, 2019) to further enhance subtle features (Kokalj and Hesse 2017). This can include hillshading, multi-directional hillshading, local relief modeling, and other methods.

Finally, DTM visualizations are combined with Digital Surface models and orthophotos derived from photogrammetric mapping to produce the final data set for each site.

3. Results and discussion

3.1. Kealakekua Bay State Historical Park, Hawai'i

Kealakekua Bay, located on the west coast of Hawai'i Island, was home to one of the Kona district's ‘royal centers’ used by the island's monarchs from CE 1600 until the early 19th century consolidation of the archipelago into a single kingdom (see McCoy 2018 for a recent review of the archaeology of royal centers). The bay is dominated by steep sea cliffs that separate the main residential area located on the Ka'awaloa Peninsula, in the north, from the religious precinct at Napo'opo'o, in the south (Fig. 5). Our first written accounts of life in Ka'awaloa are from an CE 1778-9 visit by two British ships commanded by Captain James Cook. It was at the shore in Ka'awaloa that Cook and his crew attempted to kidnap the island's king resulting in the death of Cook and four of his marines.

Standing stone architecture—enclosures, walls, platforms, terraces—is unusually dense here, perhaps denser than any other location in the islands (McCoy et al. 2021; Hommon 2014). The natural isolation of the peninsula, and the historical importance of Ka'awaloa, has helped keep both the pre- and post-contact era remains well-preserved. Today, Kealakekua Bay is managed by the Hawaii's State Parks, in partnership with the local community and tour operators who bring visitors to Ka'awaloa by boat or kayak.

Ka'awaloa presents a number of challenges for archaeologists. Survey in the Hawaiian Islands often requires dealing with thick vegetation. This occurs in locations with high rainfall and in those with lower rainfall, such as Ka'awaloa, that are frequently densely covered with mesquite tree (kiawe; *Prosopis pallida*). On older geologic substrates with sufficient rainfall, soils are well-developed and bedrock outcrops are less prevalent. In these contexts once vegetation is cleared archaeological

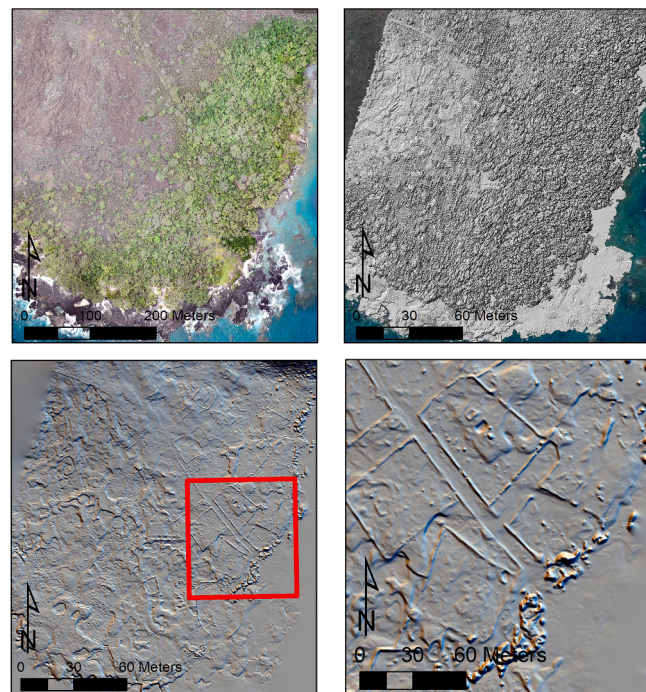


Fig. 5. Ka'awaloa Peninsula, Kealakekua Bay, Hawai'i: A) drone-derived orthoimage, B) first return lidar with tree canopy, C) bare-earth terrain model hill shade revealing extensive architectural remains, D) inset showing a close-up of central architectural remains.

features are readily identifiable. In other environments, where rainfall is lower and there are geologically young substrates, bedrock outcrops are often exposed, making it more difficult to discern built from natural features. Ka'awaloa is thickly forested on a geologically young peninsula, and for archaeological visibility this means it presents us the dual problems of archaeological features obscured by vegetation as well as a great deal of natural features (Fig. 4).

Survey was conducted in June 2019 at Ka'awaloa, an area that can only be accessed by water or via a 6.1 km hike down a steep slope. In this case, working with archaeologists from Hawai'i's State Parks and a local community group (Ho'ala Kealakekua), we hired a boat to deliver our team and equipment to a small dock at the Captain Cook Monument, the only place to access the peninsula as well as the only area from which it was possible for a drone to take off and land (Fig. 2A). Surveys were completed over a 20 ha area of the peninsula, at 40 m elevation and 2 m/s speed during transects, followed by visible light photogrammetric mapping flights using a DJI Phantom 4 Pro.

Results identified a large number of building foundations, walls, and other architectural features, none of which are observable in aerial visible light imagery (Fig. 5). We now have a dataset that allows us to distinguish wide, high walls likely built during the 19th century from the range of smaller features more likely representing the pre-European contact era (McCoy et al. 2021). The high-resolution model is particularly good for mapping the micro-topography of natural features (i.e., small lava blisters and crevasses). These allow us to distinguish the high density of domestic features in the northeast portion of the survey area from the near absence of households in the southwest. The relative density, and make up, of royal centers are especially important since the Hawaiian Islands saw the rare case where state society did not co-evolve with urbanism (Hommon 2013; Jennings and Earle 2016; Kirch 2010). Thus, the value of this type of remote sensing for archaeology in the Hawaiian Islands is not unlike other lidar-based surveys of Maya to generate a more complete picture of settlement patterns.

3.2. Mesa Verde North Escarpment, Colorado

Just north of well-known Mesa Verde National Park, Colorado, lies an extensive escarpment that today is under the jurisdiction of the Bureau of Land Management (Fig. 6). A cluster of archaeological remains within this area, known as the Knife-edge Ridge Community, was initially surveyed and cursorily recorded during a large-scale reconnaissance project by the University of Colorado in 1968 (Martin et al. 1971). The area was revisited in 2019 (Reese 2019), and several more architectural features along with a prehistoric reservoir and associated canal were identified. Ceramic assemblages associated with each structure in the Knife-edge Ridge Community suggest the area was occupied during the Pueblo II and Pueblo III periods (AD 900–1300), and was likely the most densely occupied community on the Mesa Verde North Escarpment during this time period. Despite a full-coverage pedestrian survey of the community, heavy landcover often made it difficult to accurately record the full extent of architectural rubble, and to accurately identify some types of architectural features while on-the-ground.

Lidar survey of the Knife-edge Ridge Community was conducted in July 2019 (with permission from the Bureau of Land Management – Tres Rios Field Office under Research Permit #C-79006) to explore the full extent of this dense ancestral Pueblo occupation. Data collection on the Mesa Verde North Escarpment is challenging, as there are no public access roads in the area and only a few historic logging tracks that penetrate the forest. We were fortunate to gain access to the survey area via a private ranch in the region, but we still needed to carry the large cumbersome drone and other instruments 2 km through dense forest to find suitable clearings for take-off and landing (Fig. 6). The complex terrain also created challenges for mission planning as the drone needed to follow terrain up and down the steep canyon walls in order to remain within the effective range of the lidar sensor while avoiding getting too



Fig. 6. A) Aerial photo of the North Escarpment at Mesa Verde, covered by extensive piñon-juniper forest. Mesa Verde National Park in background. B) Characteristic stone architectural remains in the North Escarpment area (Photos by Jesse Casana).

close to trees. The survey ultimately imaged over 50 ha of the study area, covering the core of the Knife-edge Ridge Community (Fig. 7).

Results of the survey produced a level of detail unattainable through pedestrian survey or image-based photogrammetry. A bare earth DTM of the results reveals more than a dozen large structures, including habitations, public architecture, and public goods (Fig. 7C-D). The most striking feature in this landscape is the prehistoric reservoir and associated canal, around which the community seems to be spatially organized. While the main canal near the reservoir is visible on the contemporary ground surface, the full extent of this water management feature is revealed in the bare earth DTM (Fig. 7C-D). The bare earth DTM shows that the canal feature extends south/southwest to several natural drainages originating from the neighboring western ridge, directly channeling water runoff to the reservoir. Furthermore, there are 2–4 smaller channels visible in the bare earth DTM that connect diagonally to the main channel, which are presumably part of a constructed drainage network to channel additional water runoff into the reservoir feature. Beyond identifying features on the surface, the bare earth DTM also enables each structure in the community to be more effectively mapped than would be easily done on the ground, enabling a straightforward comparison of their size and configuration without the hindrance of contemporary ground cover (Fig. 8).

3.3. Enfield Shaker Village, New Hampshire

Originally established in 1793, the Enfield Shaker Village grew to be one of the Shaker religious community's largest settlements by the mid-nineteenth century, with more than 300 residents and dozens of buildings spread across an area of approximately 10 ha (Stein 1992). However, like many Shaker communities, the Enfield Shaker Village declined in size gradually through the late nineteenth and early twentieth centuries and was ultimately abandoned in 1923 when the last residents moved to nearby Canterbury. After that time, many of the historic

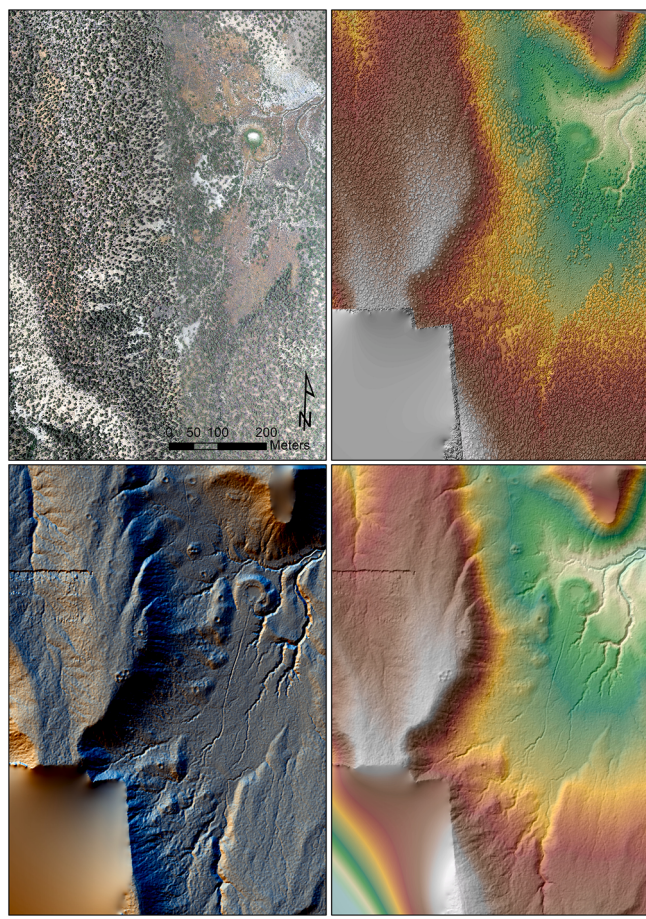


Fig. 7. Mesa Verde North Escarpment, Colorado: A) drone-derived orthoimage, B) digital surface model illustrating tree canopy as represented by first return lidar, C) bare-earth terrain model hillshade revealing numerous house compounds and a large water management system, D) resulting topographic hillshade of the Knife-edge Ridge Community.

buildings were sold, dismantled, or razed, but several significant buildings, including the “Great Stone Dwelling” erected in 1817, were left standing. Today, the Great Stone Dwelling serves as a museum and visitor center, and several of the other remaining buildings have been restored as part of a New Hampshire State Historic Park. A rich collection of historic maps, photographs, and written records reveals the location of many buildings that were once located on the site, and an archaeological excavation project, undertaken as part of a Plymouth State University field school since 2013, has uncovered portions of several buildings and a host of Shaker period artifacts (Starbuck 2016). From 2016 to 2018, our research team undertook a series of experimental surveys at the Enfield Shaker Village using a variety of aerial drone-based sensors and terrestrial geophysical instruments, documenting many building foundations and other sub-surface features in the central area of the settlement (Hill et al. 2020).

Southwest of the central area of Shaker settlement there is a large, wooded area on an adjacent mountain managed by the state as a Wildlife Management Area, throughout which traces of outlying building foundations, field walls, and other cultural features are evident—all part of an extensive outlying community of farms, workshops, and religious sites (Fig. 9). While historic photographs show that the mountain was largely deforested and used for farms and pasture in the 19th century, today the area is covered by dense mixed forest containing typical northern New England mix of deciduous maple, oak, and wild cherry, alongside evergreen stands of white pine and spruce.

We conducted a lidar survey at the site, in November 2019, designed

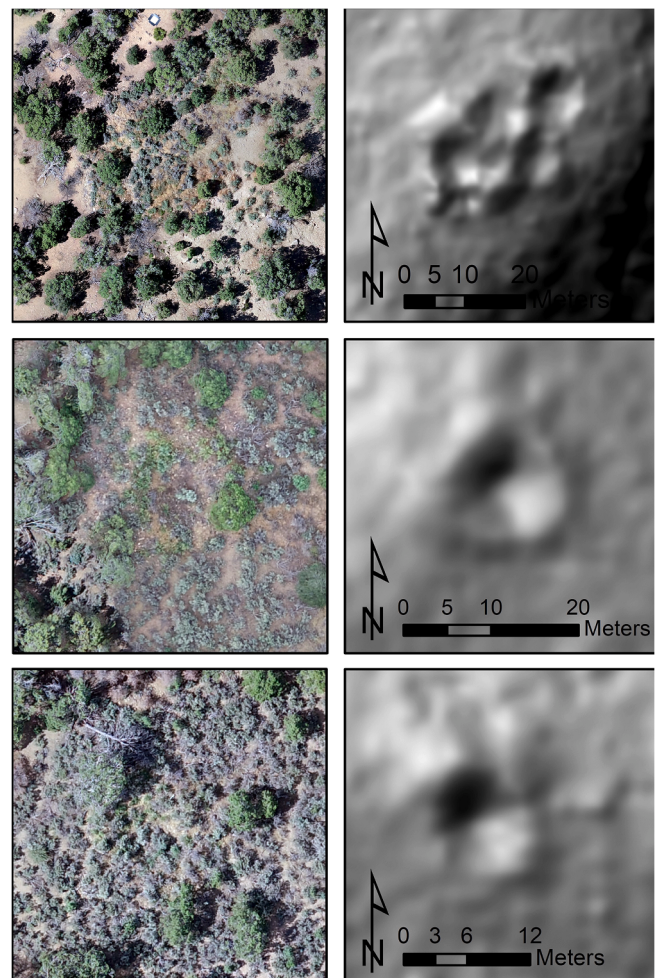


Fig. 8. Closeup of house compounds of the Knife-edge Ridge Community on the Mesa Verde North Escarpment.

to maximize potential visibility of archaeological features when the deciduous trees had lost all leaves. While a seemingly simple survey as it is nearby our lab headquarters at Dartmouth College, the survey demonstrated some limitations of our lidar system. First, the cold temperatures (17°F/-7°C) caused the drone batteries to fail repeatedly, requiring us to warm batteries ahead of time and launch the drone quickly before their temperature dropped. Even more problematic are stands of eastern white pine trees within the survey area; these trees grow to over 60 m in height, making it impractical to survey those areas, because above 60 m the lidar system would only be able to image a very narrow swath of the ground. Thus our survey results are limited to the small area of mixed deciduous forest and open field (Fig. 10). Despite these challenges, results from the Enfield Shaker Village reveal numerous archaeological features within forested areas of the site, including building foundations, canals, and water management features. A more powerful lidar sensor would enable flights at higher altitudes and thus offer the ability to map more extensive areas of sites covered by very tall trees as at Enfield.

3.4. Comparative results

After conducting drone-based lidar surveys at the three sites that are part of this study, we can offer some insights regarding the performance of the Velodyne VLP-16 lidar sensor for archaeological applications in different environmental contexts. Overall, the sensor performs reasonably well, enabling us to produce bare-earth DTMs that are substantially higher resolution than available in most public lidar datasets. In all



Fig. 9. A) Aerial photo of Enfield Shaker Village forest, Enfield, New Hampshire, covered by mixed deciduous-evergreen forest, B) characteristic stone walls from fields and architecture obscured by forest (photos by Jesse Casana).

cases, we are able to produce a bare-earth DTM with a ground sample distance of 20 cm or better, as compared to 1–2 m that is available in most public lidar datasets. There is, however, some significant variability in overall point density within individual surveys that derives from the rotation of the lidar sensor and the way in which missions are planned, as illustrated in Fig. 11. In this example from Kealakekua Bay, Hawai'i, point density of the second pulse return varies considerably across the survey area, with the highest point density immediately below the sensor, sparse coverage at survey area edges, higher density where survey transects overlap, and visible density banding due to the spinning sensor. We also see differences across sites that can be attributed to environmental contexts. At all three sites that are part of this

study we employed similar mission planning parameters, flying at 40 m elevation, 2 m/s ground speed, and a 50% overlap of adjacent transects. However, after post-processing and classifying results, we produce mean ground point densities of 39 points/meter at Mesa Verde and 35 points/meter at Enfield Shaker Village, but only 23 points/meter at Kealakekua Bay. The dense tree canopy and rich foliage in the tropical forests at Kealakekua Bay reduced penetration to the ground considerably as compared with the leaf-off deciduous forest at Enfield Shaker Village or the more arid piñon-juniper forest at Mesa Verde, signaling some caution to researchers who plan to undertake surveys in areas with dense vegetative cover and reminding us of the importance to survey in leaf-off conditions whenever possible.

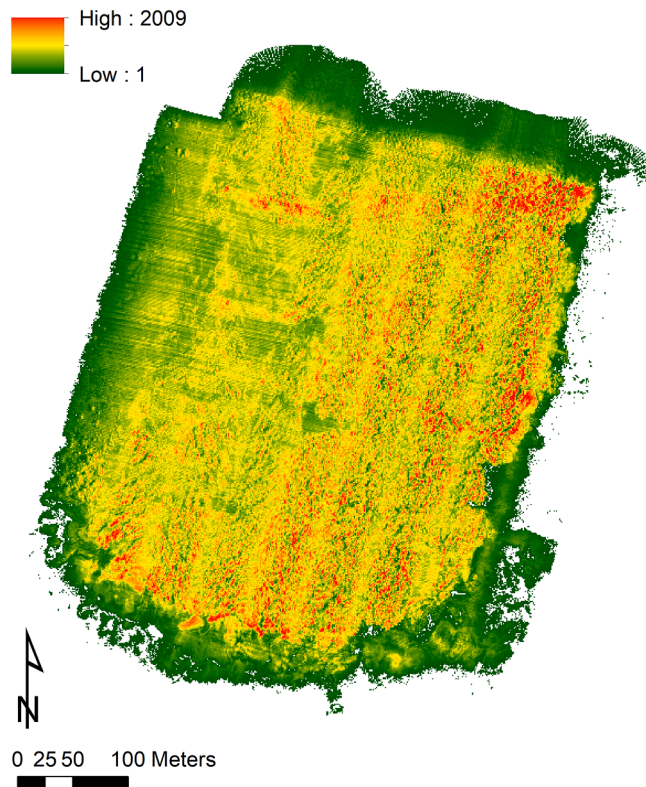


Fig. 11. Variable lidar point density from a survey at Ka'awaloa Peninsula, Kealakekua Bay, Hawai'i, resulting from the mechanics of the lidar and mission planning parameters.



Fig. 10. Results of lidar survey at Enfield Shaker Village: A) orthoimage, B) digital surface model illustrating tree canopy as represented by first return lidar, C) bare-earth terrain model hill shade revealing field walls and architectural features below forest cover.

4. Conclusions

This paper demonstrates the possibilities for archaeological discovery and documentation using drone-acquired lidar in forested and heavily vegetated areas of the world. Results from surveys in tropical forests of Hawai'i, piñon-juniper forest in Colorado, and deciduous-evergreen forest of New Hampshire consistently show the power of drone-acquired lidar to reveal many archaeological features that have topographic expression, such as building foundations, field walls, and roadways, many of which are not visible in other datasets. Moreover, by enabling us to collect much higher-resolution data than most aircraft-acquired or public lidar datasets offer, we are also able to map known archaeological features in greater detail than is otherwise possible.

With these opportunities, currently available technologies remain quite costly compared to many other field instruments, and are challenging to deploy in field settings owing to their bulky size, high rate of battery power consumption, and complex needs for mission planning. Data processing is also not a straightforward process, requiring several complex steps and multiple software platforms to move from field data acquisition to the bare-earth terrain model sought by archaeologists. However, as we have seen with rapidly developing drone technologies in other domains, it is likely that drone lidar acquisition will only become less costly and easier to achieve in the coming years.

Declaration of Competing Interest

The authors declare that they have no known competing financial interests or personal relationships that could have appeared to influence the work reported in this paper.

Acknowledgements

Funding for the field research presented herein was provided by a grant from the National Science Foundation's Archaeometry Program (#1822107) as well as from a National Endowment for the Humanities Digital Advancement grant (HAA-256086-17). Instrument and hardware acquisition were supported by a grant from the Neukom Institute for Computational Science, as well as by the Spatial Archaeometry Lab (SPARCL), the Departments of Anthropology, and the Department of Earth Sciences at Dartmouth College. Fieldwork in Hawai'i was made possible by the welcoming support of Ho'ala Kealakekua and the Hawai'i State Parks, and we are especially thankful to Tracy Tam-Sing and Mara Mulrooney for their assistance during data collection. Fieldwork in Colorado was facilitated by the Bureau of Land Management's Tres Rios Field Office, and we are grateful to Brian Yaqinto as well as to Donna Glowacki for their support of the project. Fieldwork in New Hampshire was made possible by the support of the Enfield Shaker Museum, and we are thankful to Michael O'Conner for his assistance with the project. Thanks also go to Marisa Palucis for her collaboration on instrument acquisition and testing, Dan Rockmore and Carl Renshaw for supporting the project, as well as to Elias Deeb, Adam Lewinter and other staff at the Cold Regions Research and Engineering Lab (CRREL) for their advice and consultation. Finally, we are grateful to several anonymous reviewers who provided many useful comments and suggestions on earlier drafts of this paper.

References

- Bewley, R.H., Crutchley, S.P., Shell, C.A., 2005. New light on an ancient landscape: LiDAR survey in the Stonehenge world heritage site. *Antiquity* 79, 636–647.
- Casana, J., Laugier, E.J., Hill, A.C., Blakeslee, D., 2020. A Council Circle at Etzanoa? Multi-sensor Drone Survey at an Ancestral Wichita Settlement in Southeastern Kansas. *American Antiquity* 85 (4), 761–780. <https://doi.org/10.1017/aaq.2020.49>.
- Casana, J., Wiewel, A., Cool, A., Hill, A.C., Laugier, E.J., Fisher, K., 2017. Archaeological aerial thermography in theory and practice. *Adv. Archaeol. Practice* 5 (4), 310–327. <https://doi.org/10.1017/aap.2017.23>.
- Cerrillo-Cuenca, E., 2017. An approach to the automatic surveying of prehistoric barrows through LiDAR. *Quat. Int.* 435 (PB), 135–145. <https://doi.org/10.1016/j.quaint.2015.12.099>.
- Challis, K., Forlin, P., Kinney, M., 2011. A generic toolkit for the visualization of archaeological features on airborne LiDAR elevation data. *Archaeological Prospection* 18 (4), 279–289. <https://doi.org/10.1002/arp.v18.410.1002/arp.421>.
- Chase, A.F., Chase, D.Z., Weishampel, J.F., Drake, J.B., Shrestha, R.L., Slatton, K.C., et al., 2011. Airborne LiDAR, archaeology, and the ancient Maya landscape at Caracol, Belize. *Journal of Archaeological Science* 38 (2), 387–398. <https://doi.org/10.1016/j.jas.2010.09.018>.
- Chase, A., Chase, D., Fisher, C., Leisz, S., Weishampel, J., Chase, A., 2012. Geospatial revolution and remote sensing LiDAR in Mesoamerican archaeology. *PNAS* 109 (32), 12916–12921. <https://doi.org/10.1073/pnas.1205198109>.
- Chase, A., Chase, D., Awe, J., Weishampel, J., Iannone, G., Moyes, H., et al., 2014a. Ancient Maya Regional Settlement and Inter-Site Analysis: The 2013 West-Central Belize LiDAR Survey. *Remote Sensing* 6 (9), 8671–8695. <https://doi.org/10.3390/rs6098671>.
- Chase, A.F., Chase, D.Z., Awe, J.J., Weishampel, J.F., Iannone, G., Moyes, H., Yaeger, J., Kathryn Brown, M., 2014b. The use of LiDAR in understanding the ancient maya landscape. *Adv. Archaeol. Practice* 2 (3), 208–221. <https://doi.org/10.7183/2326-3768.2.3.208>.
- Chase, A., Weishampel, J., 2016. Using Lidar and GIS to investigate water and soil management in the agricultural terracing at caracol, Belize. *Adv. Archaeol. Practice* 4 (3), 357–370. <https://doi.org/10.7183/2326-3768.4.3.357>.
- Cheng, L., Wang, Y., Chen, Y., Li, M., 2016. Using LiDAR for digital documentation of ancient city walls. *J. Cult. Heritage* 17 (C), 188–193. <https://doi.org/10.1016/j.culher.2015.04.005>.
- Due Trier, Ø., Zorteia, M., Tonning, C., 2015. Automatic detection of mound structures in airborne laser scanning data. *J. Archaeol. Sci.: Rep.* 2, 69–79. <https://doi.org/10.1016/j.jasrep.2015.01.005>.
- Evans, D., & Fletcher, R. (2015). The landscape of Angkor Wat redefined. *Antiquity*, 89 (348), 1402–1419. doi: 10.15184/agy.2015.157.
- Evans, Damian H., Fletcher, Roland J., Pottier, Christophe., Chevance, Jean-Baptiste., Soutif, Dominique., Tan, Boun Suy., Im, Sokrithy., Ea, Darith., Tin, Tina., Kim, Samnang., Cromarty, Christopher., De Greef, Stéphane., Hanus, Kasper., Bátý, Pierre., Kuszinger, Robert., Shimoda, Ichita., Boornazian, Glenn (2013). Uncovering archaeological landscapes at Angkor using lidar. *Proc. National Acad. Sci.* 110(31), 12595–12600. doi: 10.1073/pnas.1306539110.
- Fisher, C., Fernández-Díaz, J., Cohen, A., Neil Cruz, O., González, A., Leisz, S., et al., 2016. Identifying ancient settlement patterns through LiDAR in the Mosquitia Region of Honduras. *PLoS ONE*, 11(8), e0159890. doi: 10.1371/journal.pone.0159890.
- Freeland, T., Heung, B., Burley, D., Clark, G., Knudby, A., 2016. Automated feature extraction for prospection and analysis of monumental earthworks from aerial LiDAR in the Kingdom of Tonga. *J. Archaeol. Sci.* 69, 64–74. <https://doi.org/10.1016/j.jas.2016.04.011>.
- Gallagher, J.M., Josephs, R.L., 2008. Using LiDAR to detect cultural resources in a forested environment: an example from Isle Royale National Park, Michigan, USA. *Archaeological Prospection* 15 (3), 187–206. <https://doi.org/10.1002/arp.v15.310.1002/arp.333>.
- Golden, C., Murtha, T., Cook, B., Shaffer, D.S., Schroder, W., Hermitt, E.J., Alcover Firpi, O., Scherer, A.K., 2016. Reanalyzing environmental lidar data for archaeology: Mesoamerican applications and implications. *J. Archaeol. Sci.: Rep.* 9, 293–308. <https://doi.org/10.1016/j.jasrep.2016.07.029>.
- Henry, E., Shields, C., Kidder, T., 2019. Mapping the Adena-Hopewell landscape in the Middle Ohio Valley, USA: multi-scalar approaches to LiDAR-derived imagery from Central Kentucky. *J. Archaeol. Method Theory* 26 (4), 1513–1555. <https://doi.org/10.1007/s10816-019-09420-2>.
- Hill, A.C., Laugier, E.J., Reese, K.M., Ferwerda, C., Palucis, M., Casana, J. (Forthcoming). Low-Cost Drone Lidar Processing for Archaeological Prospection: finding the ground in a sea of noisy points. *Advances in Archaeological Practice*.
- Hommon, R.J., 2013. The Ancient Hawaiian State: Origins of a Political Society. New York: Oxford University Press.
- Hommon, R.J., 2014. The Kealakekua Region: salubrious core, political centre. *J. Pacific Archaeol.* 5 (2), 40–50.
- Inomata, T., Pinzón, F., Ranchos, J.L., Haraguchi, T., Nasu, H., Fernandez-Díaz, J.C., Aoyama, K., Yonenobu, H., 2017. Archaeological application of airborne LiDAR with object-based vegetation classification and visualization techniques at the Lowland Maya Site of Ceibal, Guatemala. *Remote Sensing* 9 (6), 563. <https://doi.org/10.3390/rs9060563>.
- Jennings, J., Earle, T., 2016. Urbanization, state formation, and cooperation: a reappraisal. *Curr. Anthropol.* 57 (4), 474–493.
- Johnson, K., Ouimet, W., 2014. Rediscovering the lost archaeological landscape of southern New England using airborne light detection and ranging (LiDAR). *J. Archaeol. Sci.* 43 (1), 9–20. <https://doi.org/10.1016/j.jas.2013.12.004>.
- Khan, S., Aragão, L., Iriarte, J., 2017. A UAV-lidar system to map Amazonian rainforest and its ancient landscape transformations. *Int. J. Remote Sens.* 38 (8–10), 2313–2330. <https://doi.org/10.1080/01431161.2017.1295486>.
- Kirch, P.V., 2010. How Chiefs Became Kings: Divine Kingship and the Rise of Archaic States in Ancient Hawai'i. University of California Press, Berkeley.
- Kokalj, Ž., Somrak, M., 2019. Why not a single image? Combining visualizations to facilitate fieldwork and on-screen mapping. *Remote Sensing* 11 (7), 747.
- Krasinski, K., Wygal, B., Wells, J., Martin, R., Seager-Boss, F., 2016. Detecting Late Holocene cultural landscape modifications using LiDAR imagery in the Boreal Forest, Susitna Valley, Southcentral Alaska. *J. Field Archaeol.* 41 (3), 255–270. <https://doi.org/10.1080/00934690.2016.1174764>.

- Loughlin, M., Pool, C., Fernandez-Diaz, J., Shrestha, R., 2016. Mapping the Tres Zapotes polity: the effectiveness of lidar in tropical alluvial settings. *Adv. Archaeol. Practice* 4 (3), 301–313. <https://doi.org/10.7183/2326-3768.4.3.301>.
- Macrae, S., Iannone, G., 2016. Understanding ancient maya agricultural terrace systems through lidar and hydrological mapping. *Adv. Archaeol. Practice* 4 (3), 371–392. <https://doi.org/10.7183/2326-3768.4.3.371>.
- Masini, N., Gizzi, F., Biscione, M., Fundone, V., Sedile, M., Sileo, M., Pecci, A., Lacovara, B., Lasaponara, R., 2018. Medieval archaeology under the canopy with LiDAR. the (Re)discovery of a medieval fortified settlement in southern Italy. *Remote Sensing* 10 (10), 1598. <https://doi.org/10.3390/rs10101598>.
- McCoy, M., Casana, J., Hill, A., Laugier, E., Mulrooney, M., Ladefoged, T., 2021. Unpiloted aerial vehicle acquired lidar for mapping monumental architecture: a case study from the Hawaiian Islands. *Adv. Archaeol. Practice* 9 (2), 160–174. <https://doi.org/10.1017/aap.2021.5>.
- McCoy, M.D., 2018. Celebration as a Source of Power in Archaic States: Archaeological and historical evidence for the Makahiki festival in the Hawaiian Islands. *World Archaeol.* 50 (2), 242–270.
- Mccoy, M., Asner, G., Graves, M., 2011. Airborne lidar survey of irrigated agricultural landscapes: an application of the slope contrast method. *J. Archaeol. Sci.* 38 (9), 2141–2154. <https://doi.org/10.1016/j.jas.2011.02.033>.
- McLeester, M., Casana, J., Schurr, M., Hill, A.C., Wheeler III, J.H., 2018. Detecting prehistoric landscape features using thermal, multispectral, and historical imagery analysis at midewin national tallgrass prairie, illinois. *J. Archaeolog. Sci.: Rep.* 21, 450–459. <https://doi.org/10.1016/j.jasrep.2018.08.016>.
- Murtha, T., Broadbent, E., Golden, C., Scherer, A., Schroder, W., Wilkinson, B., Zambrano, A., 2019. Drone-mounted lidar survey of maya settlement and landscape. *Latin American Antiquity* 30 (3), 630–636. <https://doi.org/10.1017/laq.2019.51>.
- Opitz, R., Cowley, D., 2013. *Interpreting Archaeological Topography: Airborne Laser Scanning, 3D Data and Ground Observation*. Oxbow Books, Oxford.
- Opitz, R., Ryzewski, K., Cherry, J., Moloney, B., 2015. Using airborne LiDAR Survey to explore Historic-era archaeological landscapes of Montserrat in the Eastern Caribbean. *J. Field Archaeol.* 40 (5), 523–541. <https://doi.org/10.1179/2042458215Y.0000000016>.
- VanValkenburgh, P., Cushman, K.C., Butters, L.J.C., Vega, C.R., Roberts, C.B., Kepler, C., Kellner, J., 2020. Lasers without lost cities: using drone lidar to capture architectural complexity at Kuelap, Amazonas, Peru. *Journal of Field Archaeology* 45 (sup1), S75–S88. <https://doi.org/10.1080/00934690.2020.1713287>.
- Prufer, K., Thompson, A., Kennett, D., 2015. Evaluating airborne LiDAR for detecting settlements and modified landscapes in disturbed tropical environments at Uxbenká, Belize. *J. Archaeol. Sci.* 57, 1–13. <https://doi.org/10.1016/j.jas.2015.02.013>.
- Randall, A., 2014. LiDAR-aided reconnaissance and reconstruction of lost landscapes: An example of freshwater shell mounds (ca. 7500–500 cal b.p.) in northeastern Florida. *J. Field Archaeol.* 39 (2), 162–179. <https://doi.org/10.1179/0093469014Z.00000000080>.
- Riley, M., Tiffany, J., 2014. Using LiDAR data to locate a Middle Woodland enclosure and associated mounds, Louisa County, Iowa. *J. Archaeol. Sci.* 52, 143–151. <https://doi.org/10.1016/j.jas.2014.07.018>.
- Risbøl, O., Gustavsen, L., 2018. LiDAR from drones employed for mapping archaeology – potential, benefits and challenges. *Archaeological Prospection* 25 (4), 329–338. <https://doi.org/10.1002/arp.v25.410.1002/arp.1712>.
- Rosenswig, R., Lopez-Torrijos, R., Antonelli, C., Mendelsohn, R., 2013. Lidar mapping and surface survey of the Izapa state on the tropical piedmont of Chiapas, Mexico. *J. Archaeol. Sci.* 40 (3), 1493–1507. <https://doi.org/10.1016/j.jas.2012.10.034>.
- Starbuck, D., 2016. Enfield shaker village: summer 2016 field school. *New Hampshire Archaeological Society Newsletter* 32, 1–2.
- Stein, S., 1992. *Shaker Experience in America*. Yale University Press, New Haven, CT.
- Stenborg, P., Schaaf, D., Figueiredo, C., 2018. Contours of the past: LiDAR data expands the limits of late pre-columbian human settlement in the Santarém Region, Lower Amazon. *J. Field Archaeol.* 43 (1), 44–57. <https://doi.org/10.1080/00934690.2017.1417198>.
- Venter, M., Shields, C., Cuevas Ordóñez, M., 2018. Mapping Matacanela: The complementary work of lidar and topographical survey in southern Veracruz, Mexico. *Ancient Mesoamerica* 29 (1), 81–92. <https://doi.org/10.1017/S0956536117000128>.
- Yaeger, J., Brown, M., Cap, B., 2016. Locating and dating sites using lidar survey in a mosaic landscape in Western Belize. *Adv. Archaeol. Practice* 4 (3), 339–356. <https://doi.org/10.7183/2326-3768.4.3.339>.